



Development of triethanolamine functionalized-anion exchange membrane for adsorptive removal of methyl orange from aqueous solution

Muhammad Imran Khan*, Jinzhan Su, Liejin Guo*

State Key Laboratory of Multiphase Flow in Power Engineering (MPFE), International Research Centre for Renewable Energy (IRCRE), Xi'an Jiaotong University, 28 West Xianning Road, Xi'an 710049, China, emails: raويمranishaq@gmail.com (M.I. Khan), lj-guo@mail.xjtu.edu.cn (L. Guo), j.su@xjtu.edu.cn (J. Su)

Received 6 April 2020; Accepted 22 August 2020

ABSTRACT

In this work, the fabrication of homogenous triethanolamine functionalized-anion exchange membrane (AEM) was carried out by incorporating triethanolamine into brominated poly(2,6-dimethyl-1,4-phenyleneoxide) (BPPO) matrix via solution casting method. The successful fabrication of triethanolamine functionalized-AEM was confirmed by Fourier transform infrared (FTIR) spectroscopy. The fabricated triethanolamine functionalized-AEM showed higher thermal stability. Moreover, the prepared AEM showed homogeneous morphology. The fabricated AEM was utilized for the adsorptive discharge of methyl orange (MO) from aqueous solution at room temperature. The effect of several parameters including contact time, amount of the fabricated AEM (adsorbent), and temperature on the percentage discharge of methyl orange from aqueous solution were evaluated. The percentage discharge of MO from aqueous solution was enhanced with the contact time, amount of the fabricated AEM (adsorbent), and temperature. Kinetic models including pseudo-first-order, pseudo-second-order, Elovich, liquid film diffusion, modified Freundlich equation, and Bangham equation were utilized to study adsorption kinetics for the discharge of MO from aqueous solution. Results showed that experimental data for adsorption of methyl orange from aqueous solution onto the prepared AEM followed the pseudo-second-order kinetic model.

Keywords: Anion exchange membrane; Methyl orange; Adsorption; BPPO; Triethanolamine; Pseudo-second-order model

1. Introduction

Environmental protection has led the scientific community to appoint in an endeavor for nature conservancy. It has been done by utilizing new ecofriendly production methods and impairs rebuilding activities to overturn established eco-devastating trends from the last few decades. The general idea to become “greener” is based generally on control, wherever possible, viable employ of non-renewable assets and devaluation of pollution. Water and air are the most crucial targets in this respect. Water and air pollution is threatening the health of the population and shows a high

endanger hazard for all animals. There are several kinds of pollution attracting on water. There are many methods have been matured that should still be bettered to try to discharge these poisons from freshwater and ground sources. Water is a colorless, tasteless, odorless, and transparent natural solvent. It contains toxic dyes [1]. As a matter of fact, dyes are removed into the water and into the environment by several industries working, for instant, in the paper, textiles, cosmetics, and leather sectors to name just a few, due to dyes are part of the chemicals employed to impart special properties to their products [2,3]. Dyes are of various kinds based on their chemical nature [4]. Usually dyes

* Corresponding authors.

are classified into cationic, anionic, and non-ionic (neutral) molecules based on ionization property in aqueous solution. These are stable to light and aerobic digestion and resistant to biological degradation.

In industrial areas, organic dyes are one of the major pollutants. Because of its inertness, the discharge of dyes from water is not easy. Methyl orange is a bourgeois dye that is largely utilized for textile coloring. This is accredited to be carcinogenic and mutagenic in nature [5]. In recent years, several techniques have been developed for the discharge of dye and water treatment. Some suitable techniques are reverse osmosis [6], ion exchange membrane [7], flocculation [8], bacterial action, adsorption [9,10], photocatalytic degradation [11], etc. Adsorption is considered as one of the simplest one because of its manageable operation and cheapness among them [12]. Adsorption is the most comprehensive and the best technique for the discharge of azo dyes from water and industrial wastewaters due to its capability to discharge like these dyes at any concentration, easy to design, and a relatively cheap [13,14].

Current research has been scrutinized by employing adsorption/ion exchange to water polluted with a broad range of reactive dyes. Because of their exclusive chemical properties, enormous quantity of applied reactive dyes frequently end up in wastewaters and this has aroused us to find the demand for enough treatment methods. For instant [15], several commercial adsorbents (zeolites, polystyrene resins, ion exchangers, and granulated ferric hydroxide) were used for the discharge of reactive dye and found that anion exchange resins were the most adequate adsorbents. A follow-up work by the same researchers gave appropriate information for the benefits of packed-bed operation, such as the form of resin regeneration [16]. Nonetheless, eminent commercial ion exchangers are in the form of porous particles and their packed-bed operation for flow process usually possess some deficiencies including flow channeling, high pressure drop, low accessible flow rate, slow pore diffusion, etc. For removing the above-mentioned problems, ion exchange membrane is a magnificent substitute. It could not only breakdown the mass transfer issues for packed beds but also indicate the characteristics of easier scale-up design (either using a larger membrane area or staking more membranes together). Hence, ion exchange membrane should be a magnificent choice for adsorption of dyes and the related accomplishment should be adequately studied. Nonetheless, the utilization of ion exchange membranes for the discharge of dye from wastewater has been ignored from long time.

Our previous research showed the utilization of several commercial anion exchange membranes (AEMs) for adsorptive discharge of dyes from aqueous solution at room temperature [17–20]. In the present work, the triethanolamine functionalized-AEM was prepared by introducing triethanolamine into brominated poly(2,6-dimethyl-1,4-phenyleneoxide) (BPPO) matrix via solution casting method. The fabricated AEM was characterized in term of Fourier transform infrared spectroscopy (FTIR), thermal gravimetric analysis (TGA), and scanning electron microscopy (SEM). The prepared AEM was employed for adsorptive removal of methyl orange (MO) from aqueous solution at room temperature. The effect of contact time, amount of AEM (adsorbent), and temperature on the percentage

discharge of methyl orange from aqueous solution was investigated. Adsorption kinetics for the discharge of methyl orange from aqueous solution was also evaluated in detail.

2. Experimental

2.1. Materials

Poly(2,6-dimethyl-1,4-phenyleneoxide) (PPO) was kindly supplied by Sigma-Aldrich Chemicals (Germany). Triethanolamine, chlorobenzene, ethanol, chloroform, *N*-methyl-2-pyrrolidone (NMP), 2,2'-Azo-bis-isobutyro nitrile (AIBN), *N*-bromo-succinimide (NBS), and methyl orange (MO) were kindly provided by Sinopharm Chemical reagent Co., Ltd., China and employed as received. Distill water was employed throughout this work.

2.2. Fabrication of BPPO

Fabrication has been described [21] (Fig. 1). Typically, 6 g of PPO (50 mmol) was dissolved into 50 mL of chlorobenzene in a round bottom flask containing a magnetic stirrer and reflexed condenser. NBS (4.45 g, 25 mmol), and AIBN (0.25 g, 1.5 mmol) were added and the solution was stirred at 135°C for 3 h. After cooling at 25°C, the reaction mixture was poured into an excess of ethanol to precipitate the polymer. The polymer was filtered, washed with ethanol, re-dissolved into 60 mL chloroform, and precipitated into an excess of ethanol solution. The polymer was collected as a light-yellow powder and dried under vacuum for 2 d at 40°C to attain BPPO with bromination ratio of 75%.

2.3. Fabrication of AEM

In this article, the fabrication of triethanolamine functionalized-AEM was carried out by utilizing solution casting method as reported in the literature [22–27]. Initially, 8% (w%) solution of BPPO was prepared by dissolving 0.8 g of BPPO into 10 mL of NMS. Triethanolamine functionalized-AEM was prepared by adding 0.45 g of triethanolamine into casting solution. The reaction mixture was stirred overnight at 40°C and then casted onto a glass plate at 60°C for 1 d. Membrane was peeled off from glass plate and cleaned with distil water. The chemical structure of the triethanolamine functionalized-AEM is also shown in Fig. 1.

2.4. Characterization

2.4.1. Instrumentations

¹H NMR (DMX 300 NMR spectrometer operating at 300 MHz) was utilized to confirm bromination of PPO. The successful fabrication of AEM was confirmed by using attenuated total reflectance (ATR) with FTIR spectrometer (Vector 22, Bruker) in the range of 4,000–400 cm⁻¹. Field emission scanning electron microscopy (FE-SEM, Sirion200, FEI Company, Massachusetts, MA, USA) was employed to investigate morphology of the prepared AEM in detail. Similarly, the Shimadzu TGA-50H analyzer (Kyoto, Japan) under nitrogen flow with a heating rate of 10°C/min within the temperature range of 25°C–800°C was employed to study thermal stability of the developed AEM.

2.4.2. Adsorption procedure

Batch adsorption of MO from aqueous solution onto the fabricated triethanolamine functionalized-AEM was carried as reported in the literature [18–20,28–30]. In a typical procedure, known amount of the triethanolamine functionalized-AEM was soaked into 50 mL of dye aqueous solution of known concentration at room temperature. The flasks were shaken at a constant speed of 120 rpm. The flasks were withdrawn from shaker at predetermined time, and residual MO concentration in the aqueous solution was calculated by measuring the absorbance of the supernatant by UV/VIS spectrophotometer (UV-2550, SHIMADZU) at wavelength ($\lambda_{\max} = 464$ nm for MO) that corresponds to the maximum absorbance of sample. Dye concentration in the reaction mixture was measured from the calibration curve. Adsorption experiments were conducted by varying contact time from 300 to 2,880 min with different time intervals, membrane dose from 0.01 to 0.05 g, and temperature from 298 to 333 K. The concentration of dye solution used was 50 mg/L. The amount of MO adsorbed onto the triethanolamine functionalized-AEM at time t , was determined by below relationship.

$$q_t = \frac{C_0 - C_t}{W} \times V \quad (1)$$

where C_0 and C_t represents the concentration of MO at initial state and at time t , respectively. Similarly V and W are

volume of MO aqueous solution and weight of the prepared membrane, respectively.

3. Results and discussion

3.1. Fabrication of BPPO

BPPO was synthesized by bromination of commercially available PPO by using NBS as a brominating agent and AIBN as an initiator. The bromination can occur either at benzylic position or at the aromatic ring depending on the reaction condition and reagents [21,31]. In this research, it took place at benzylic position of PPO in refluxing chlorobenzene solution at 135°C using above-mentioned conditions. The structure and degree of bromination (DB) of synthesized BPPO were investigated by ^1H NMR spectroscopy. ^1H NMR spectrum of BPPO is represented in Fig. 2. It has been observed that the characteristic benzyl bromide group was located at 4.3 ppm. The degree of bromination (DB) calculated from integral area ratio between benzyl bromide group and unreacted benzyl signal at 2.1 ppm was 75%.

3.2. FTIR and TGA tests

The successful fabrication of the triethanolamine functionalized-AEM was proved by FTIR spectroscopy. FTIR spectrum of pure BPPO and triethanolamine functionalized-AEM is shown in Fig. 3a. The peak at 750 cm^{-1} is associated to C–Br stretching in the pure BPPO membrane [32,33]. After reaction

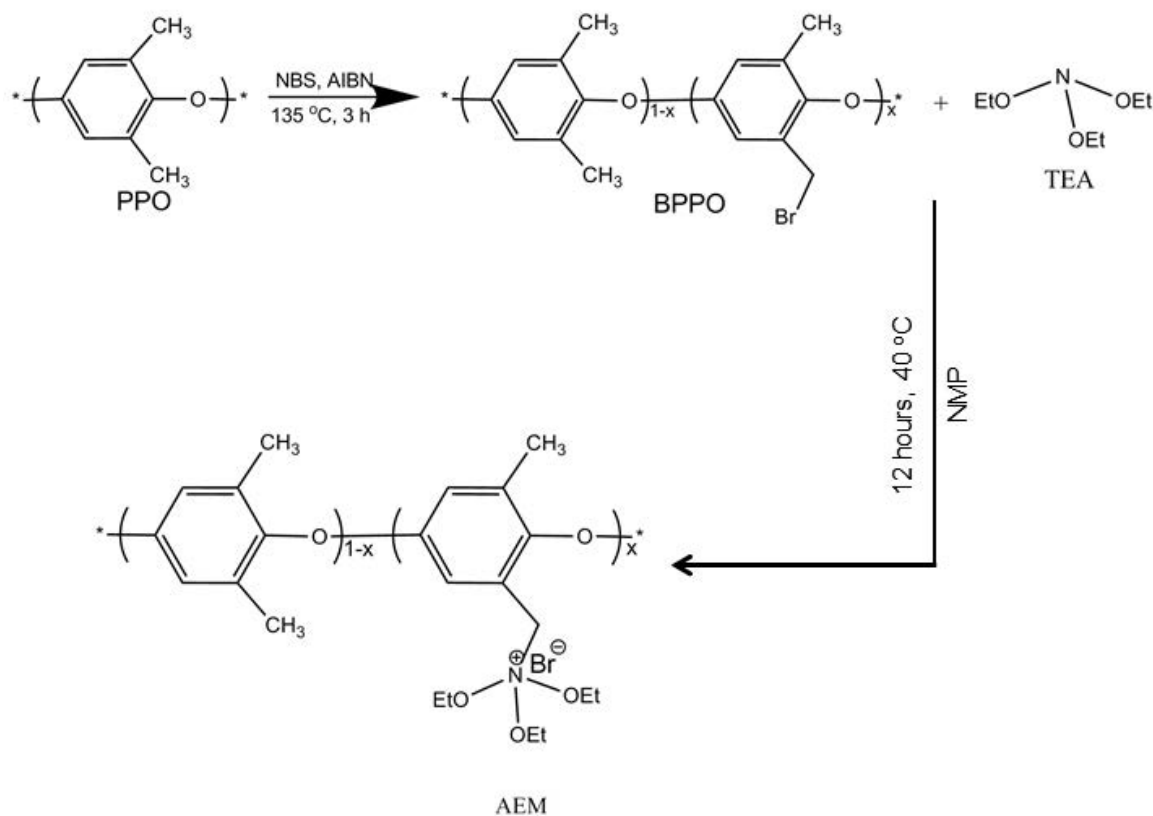


Fig. 1. Fabrication of brominated poly(2,6-dimethyl-1,4-phenyleneoxide) and triethanolamine functionalized-AEM.

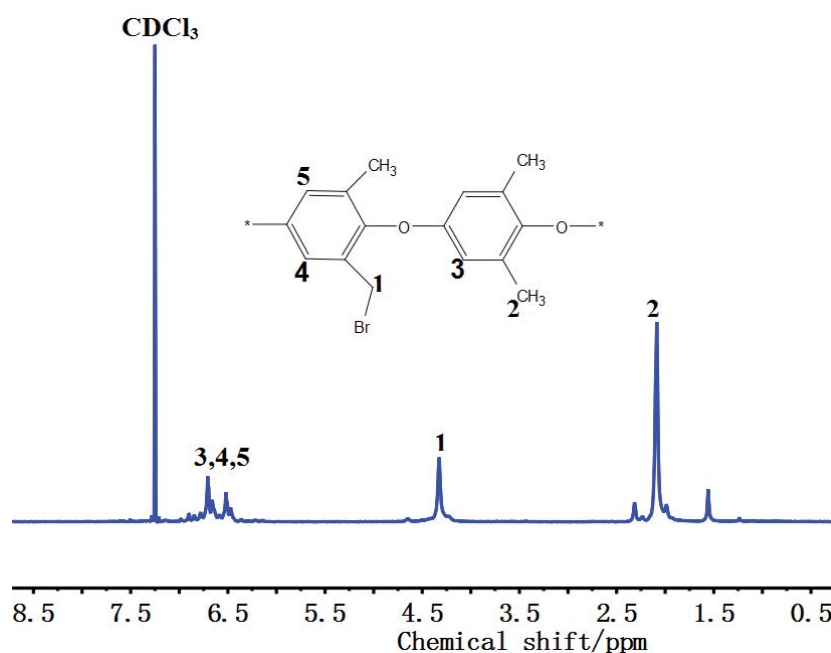


Fig. 2. ^1H NMR spectra of BPPO representing the successful bromination of PPO.

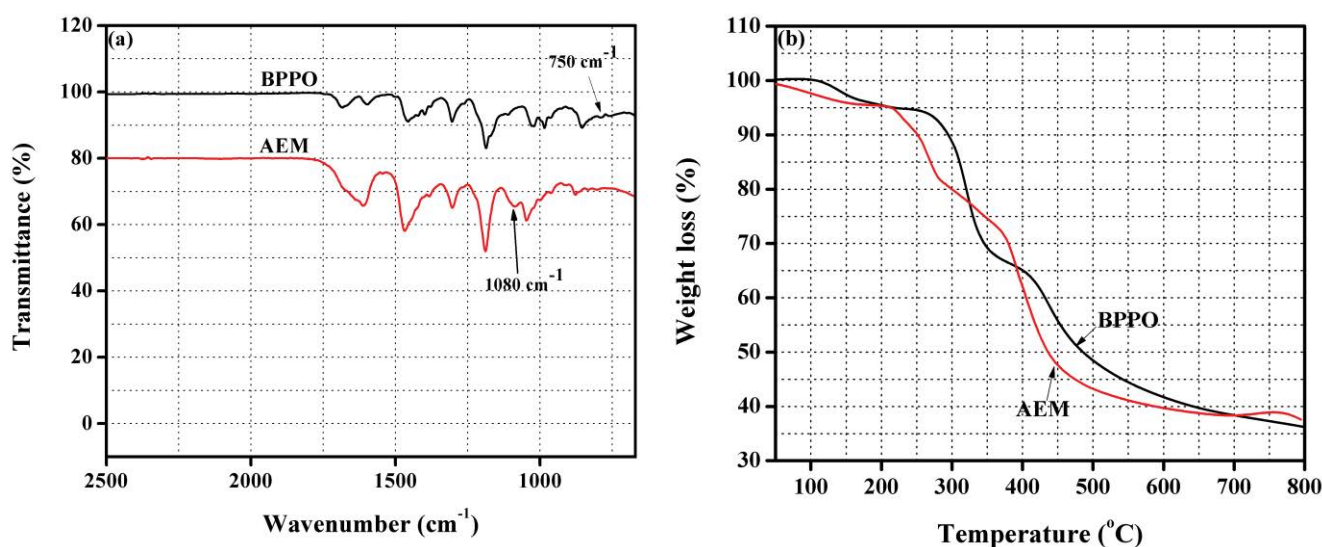


Fig. 3. (a) FTIR spectrum of pure brominated poly(2,6-dimethyl-1,4-phenyleneoxide) (BPPO) and triethanolamine functionalized-AEM and (b) thermogravimetric analysis curves of pristine BPPO and triethanolamine functionalized-AEM.

of triethanolamine with BPPO, the signal for C–Br at 750 cm^{-1} in the triethanolamine functionalized-AEM was disappeared [32,34]. In the prepared membrane, the new peak at $1,080\text{ cm}^{-1}$ showed to the successful reaction of triethanolamine with BPPO which is same as reported in our previous work [28]. It is due to the C–N stretching vibration in the fabricated AEM. It is absent in the spectrum of pure BPPO membrane. These evidences showed successful fabrication of the triethanolamine functionalized-AEM.

Thermogravimetric analysis curves of pure BPPO and triethanolamine functionalized-AEM is shown in Fig. 3b. The weight loss of pure BPPO membrane and the

prepared triethanolamine functionalized-AEM took place into three steps which corresponds to evaporation of adsorbed water, thermal deamination and thermal oxidation of the polymer architecture. Around 80°C – 130°C , the evaporation of adsorbed water from polymer matrix took place which is first stage of weight loss. The second step of weight loss around 230°C – 240°C took place is due to degradation of quaternary ammonium group [22,23,33]. The final weight loss took place around 415°C is because of degradation of the polymer architecture. These evidences showed good thermal stability of the triethanolamine functionalized-AEMs.

3.3. Morphology

Fig. 4 depicts morphology of surface and cross-section of the fabricated triethanolamine functionalized-AEMs. It was studied by utilizing field emission scanning electron microscope (FE-SEM, Sirion200, FEI Company, USA). The surface and cross-section of the fabricated triethanolamine functionalized-AEMs is free from any crack or hole representing its homogeneous structure. Further, Figs. 5a and b show color change of the prepared AEM before and after adsorption of MO from aqueous solution onto the triethanolamine functionalized-AEM. Moreover, it also represents adsorptive discharge of methyl orange from aqueous solution Figs. 5c and d.

3.4. Effect of operating parameters

The influence of contact time, amount of the prepared AEM (adsorbent), and temperature on the percentage discharge of methyl orange from aqueous solution have been studied. The detail discussion is given below.

3.4.1. Effect of contact time

Fig. 6a denotes the effect of contact time on adsorption of MO from aqueous solution onto the prepared AEM. It was investigated keeping the shaking speed (120 rpm), concentration of adsorbate (50 mg/L), amount of the prepared AEM (adsorbent) constant at room temperature. The attained results represent that adsorption of MO from aqueous solution onto the prepared AEM was enhanced from 52% to 97% with contact time. The equilibrium was attained in 48 h and this optimum contact time was utilized for further investigation. It can be seen that the percentage discharge of MO from aqueous solution by the prepared AEM was fast in the initial stage due to presence of a large number of empty sites onto the surface

of the prepared AEM during the initial stage. After this, the adsorption of dye did not enhanced because of the occupation of active sites onto adsorbent (AEM) surface and non-availability of active sites for further adsorption of dye ions [35]. Similar results have been reported in our previous research [17–20,30].

3.4.2. Effect of amount of the prepared AEM

Fig. 6b depicts the influence of the amount of the prepared AEM (adsorbent) on the percentage discharge of MO from aqueous solution at ambient temperature. It was investigated keeping contact time, concentration of adsorbate (50 mg/L), shaking speed and temperature constant. The attained results indicated that the percentage discharge of MO from aqueous solution was enhanced with increasing the amount of the prepared AEM (adsorbent). The percentage discharge of MO from aqueous solution was fastly increased from 52% to 96% with increase in the amount of adsorbent (AEM) from 0.01 to 0.03 g. It was due to increase in number of available active sites with enhancing the amount of the prepared AEM. With increase in the amount of adsorbent from 0.03 to 0.05 g, the percentage discharge of MO was increased from 96% to 97% from aqueous solution which was very small change. It could be because of the saturation of binding sites [36]. Therefore, the amount of AEM (adsorbent) for further study was 0.03 g. Similarly results have been previously reported in the literature [17,18].

3.4.3. Effect of temperature

Fig. 6c represents the influence of temperature on adsorption of MO from aqueous solution onto the prepared AEM. It was investigated keeping the contact time, amount of the AEM, stirring speed, solution volume, and concentration (50 mg/L) constant. The percentage discharge of MO from aqueous solution was enhanced from 97% to 98.50%

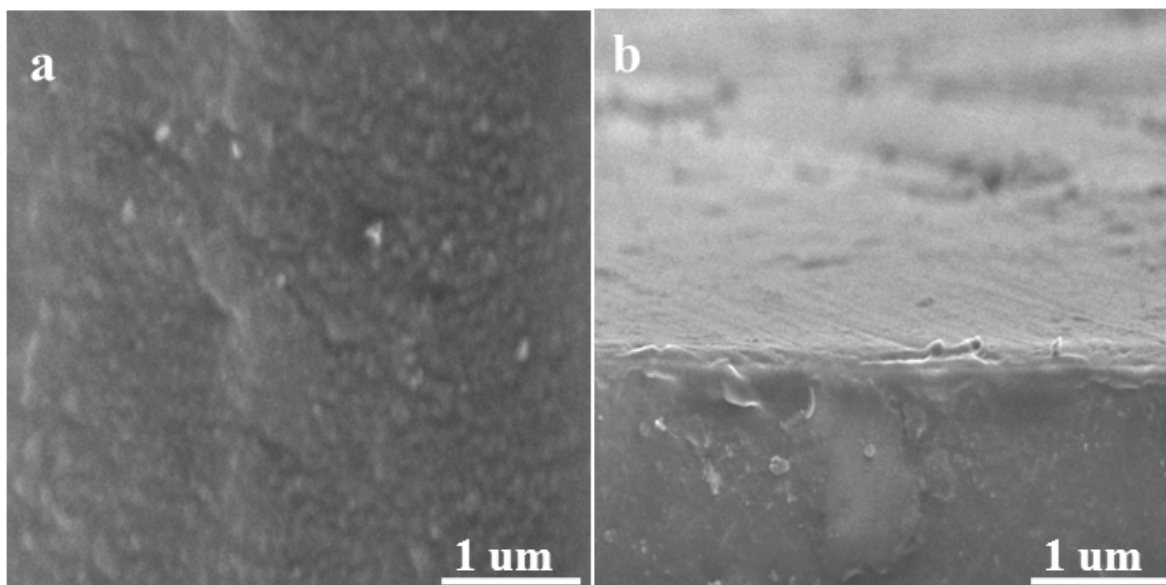


Fig. 4. (a) SEM image of surface and (b) SEM image of cross-section of the triethanolamine functionalized-AEM.

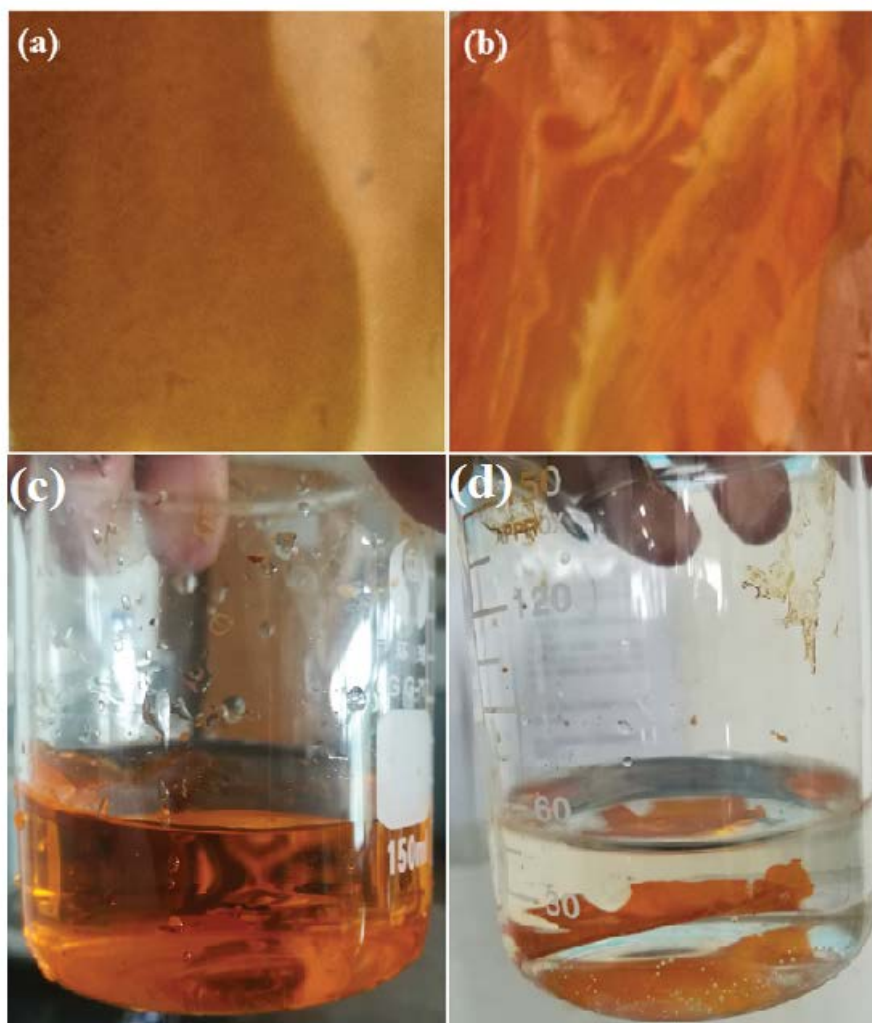


Fig. 5. (a) Triethanolamine functionalized-AEM before adsorption of methyl orange onto it, (b) triethanolamine functionalized-AEM after adsorption of methyl orange onto it, (c) MO aqueous solution before adsorption of methyl orange onto triethanolamine functionalized-AEM, and (d) MO aqueous solution after adsorption methyl orange onto triethanolamine functionalized-AEM.

with enhancing temperature from 298 to 333 K. It represents that adsorption of MO from aqueous solution onto the prepared AEM was an endothermic process.

3.5. Adsorption kinetics

Many adsorption models were employed to study the controlling mechanism of adsorption process such as chemical reaction and diffusion control.

3.5.1. Pseudo-first-order model

The linearized form of the Lagergren Pseudo-first-order rate equation is represented as [37,38]:

$$\log(q_e - q_t) = \log q_e - \frac{k_1 t}{2.303} \quad (2)$$

where q_e and q_t shows the adsorbed amount of dye at equilibrium and time t respectively and k_1 (1/min) is rate

constant of pseudo-first-order model. Fig. 7a depicts the plot of $\log(q_e - q_t)$ vs. time for adsorption of MO from aqueous solution onto the prepared AEM. The values of k_1 and q_e for adsorption of MO onto the prepared anion exchange were calculated from slope and intercept of the plot and are given in Table 1. The plot is linear, however, the linearity of the curve does not necessarily assure the mechanism due to the inherent disadvantage of correctly estimating equilibrium adsorption capacity [17,38]. From Table 1, it has been observed that there is a large difference between experimental adsorption capacity ($q_{e,exp}$) and calculated adsorption capacity values ($q_{e,cal}$). Moreover, the value of correlation coefficient (R^2) was 0.732. Hence, the pseudo-first-order model does not explain the rate process.

3.5.2. Pseudo-second-order model

The linearized form of pseudo-second-order kinetic model is shown as [39–41]:

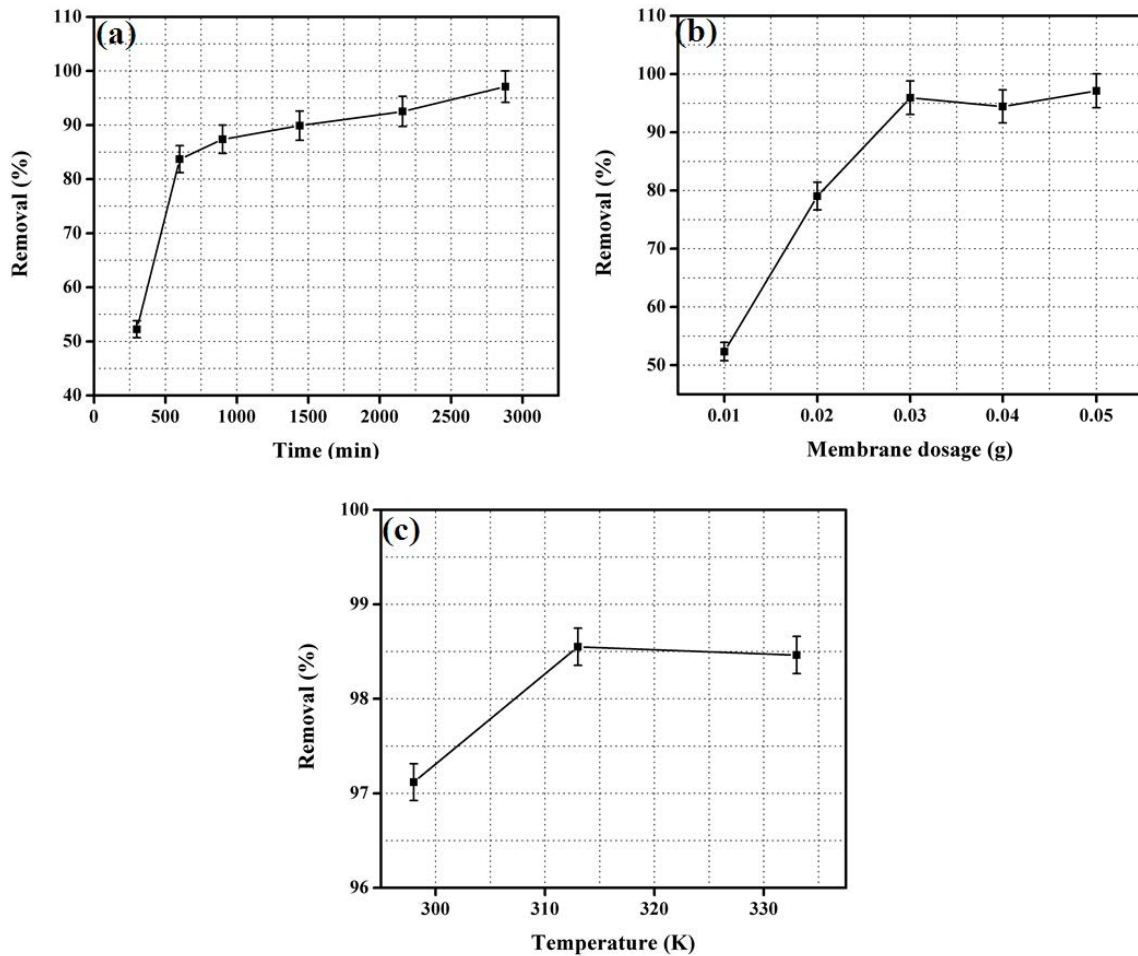


Fig. 6. Effect of (a) contact time, (b) amount of the prepared anion exchange membrane (adsorbent) and (c) temperature on the percentage removal of MO from aqueous solution by the prepared triethanolamine functionalized-AEM.

$$\frac{t}{q_t} = \frac{1}{k_2 q_e^2} + \frac{t}{q_e} \quad (3)$$

where k_2 (g/mg min) is the rate constant of pseudo-second-order model. Fig. 7b shows the plot of t/q_t vs. t for adsorption of MO from aqueous solution onto the prepared AEM. Herein, adsorption capacity (q_e) was measured from slope of plot and attained value is given in Table 1. This value of adsorption capacity was in good agreement with the experimental value (19.42 mg/g). Moreover, the value of correlation coefficient was close to unity ($R^2 > 0.99$) which showed that experimental data for adsorption of MO from aqueous solution onto the prepared AEM obeyed pseudo-second-order model.

3.5.3. Elovich model

The most interesting model to explain the activated chemisorption is the Elovich model [42]:

$$q_t = \frac{1}{\beta} \ln(\alpha\beta) + \frac{1}{\beta} \ln t \quad (4)$$

where α (mg/g min) and β (g/mg) are constant. The parameter α is considered as initial adsorption rate (mg/g min) and β is related to the extent of surface coverage and activation energy for chemisorption. Fig. 7c depicts graphical representation of Elovich model for adsorption of MO from aqueous solution onto the prepared AEM. The values of α and β were calculated from intercept and slope of the plot of t vs. q_t and are given in Table 1. The value of correlation coefficient (R^2) was 0.759 which is lower than that of pseudo-second-order model.

3.5.4. Liquid film diffusion model

The migration of dye through liquid film from bulk solution to the exterior surface of adsorption sites may play a crucial role in calculating adsorption rate. For determination of potential rate-controlling step, the data for adsorption of MO onto the prepared AEM was studied by employing liquid film diffusion model. The liquid film model is given as [43]:

$$\ln\left(1 - \frac{q_t}{q_e}\right) = -K_{fd} t \quad (5)$$

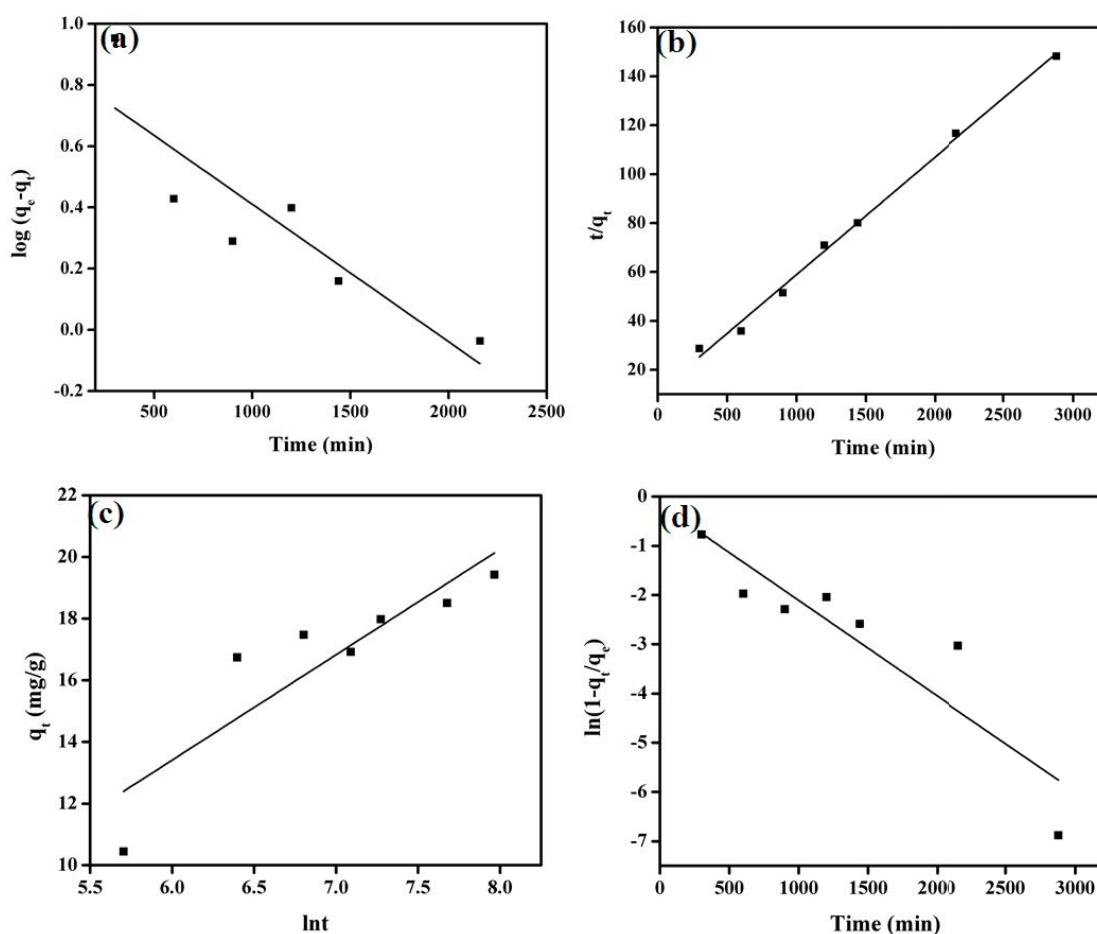


Fig. 7. (a) Pseudo-first-order kinetics, (b) pseudo-second-order kinetics, (c) Elovich model and (d) liquid film diffusion model for adsorption of MO onto the prepared triethanolamine functionalized-AEM.

where K_{fd} shows liquid film diffusion rate constant. The plot of $\ln(1 - q_t/q_e)$ vs. time for adsorption of MO from aqueous solution onto the prepared anion exchange is a straight line for liquid film diffusion model and is shown in Fig. 7d. Herein, Table 1 shows the value of K_{fd} calculated from slope of the linear plot. The value of correlation coefficient (R^2) was 0.789 which is lower than pseudo-second-order model. It showed that liquid film diffusion model cannot be sufficient to explain experimental data. Therefore, the explanation of experimental data for adsorption of MO onto the prepared AEM from aqueous solution required other models.

3.5.5. Modified Freundlich equation

The modified Freundlich equation was originally developed by Kuo and Lotse [17].

$$q_t = kC_0 t^{1/m} \quad (6)$$

where q_t represents the amount of adsorbed dye (mg/g) at time t , k shows the apparent adsorption rate constant (L/g min), C_0 depicts the initial dye concentration (mg/L), t shows the contact time (min), and m represents the Kuo–Lotse constant. The values of k and m were utilized to

investigate the influence of dye surface loading and ionic strength on adsorption process. Linear form of modified Freundlich equation is expressed as:

$$\ln q_t = \ln(kC_0) + \frac{1}{m} \ln t \quad (7)$$

Fig. 8a shows the graphical representation of modified Freundlich equation for adsorption of MO from aqueous solution onto the prepared AEM. The endowments m and k were calculated from slope and intercept of plot of $\ln t$ vs. $\ln q_t$ and are shown in Table 1. The value of correlation coefficient (R^2) for adsorption of MO onto the prepared AEM was 0.701. It showed that experiment data for adsorption of MO onto the prepared AEM was not fitted well to modified Freundlich equation.

3.5.6. Bangham equation

Bangham equation [17] is expressed as:

$$\log\left(\frac{C_0}{C_0 - q_t m}\right) = \log\left(\frac{k_0 m}{2.303V}\right) + \alpha \log t \quad (8)$$

Table 1

Pseudo-first-order model, pseudo-second-order model, Elovich, liquid film diffusion model, modified Freundlich equation, and Bangham equation rate constants (q_e (mg/g), k_1 (1/min), k_2 (g/mg min), α (mg/g min), β (g/mg), K_{fd} (1/min), k (L/g min), and k_0 (mL/g/L))

Kinetic models		Parameters	
Pseudo-first-order model	q_e (exp)	19.42	
	q_e	$k_1 \times 10^{-4}$	R^2
	7.24	4.49	0.732
Pseudo-second-order model	q_e	$k_2 \times 10^{-4}$	R^2
	20.79	2.13	0.995
Elovich model	α	β	R^2
	0.44	0.29	0.759
Liquid film diffusion model	$K_{fd} \times 10^{-3}$	C_{fd}	R^2
	1.94	-0.17	0.789
Modified Freundlich equation	m	k	R^2
	4.27	0.064	0.701
Bangham equation	$k_0 \times 10^{-3}$	α	R^2
	1.28	0.24	0.701

where V is volume of solution (mL), C_0 is initial concentration of dye solution (mg/L), q_t is amount of dye adsorbed (mg/g) at time t , m is weight of adsorbent used (g/L). α (<1) and k_0 (mL/(g/L)) are constants. Fig. 8b shows the plot of $\log\log(C_0/C_0 - mq_t)$ vs. $\log t$ for adsorption of MO onto the prepared AEM from aqueous solution. The values of α and m were calculated from slope and intercept of straight line and are given in Table 1. The double logarithmic plot did not give linear curve for adsorption of MO from aqueous solution onto the prepared AEM denoting that the diffusion of adsorbate into pores of the adsorbent is not the only rate-controlling step [44,45]. It may be that both film and pore diffusion were significant to different extent in adsorption of MO onto the prepared AEM from aqueous solution.

4. Conclusions

In this research, triethanolamine functionalized-AEM was successfully fabricated by utilizing solution casting method. The successful fabrication of AEM was confirmed by FTIR

spectroscopy. The fabricated AEM exhibited homogeneous structure as confirmed by SEM. Moreover, it exhibited good thermal stability. The developed AEM was utilized for the discharge of methyl orange from aqueous solution at room temperature. The percentage discharge of methyl orange from aqueous solution by AEM was enhanced with contact time, amount of the fabricated AEM (adsorbent), and temperature. Kinetic study showed that experimental data for adsorption of methyl orange from aqueous solution onto the prepared AEM followed pseudo-second-order model. Therefore, the fabricated triethanolamine functionalized-AEM could be utilized as a good adsorbent for the discharge of methyl orange from aqueous solution at room temperature.

Acknowledgment

The authors are highly thankful to the financial support from the Basic Science Center Program for Ordered Energy Conversion of the National Natural Science Foundation of China (51888103).

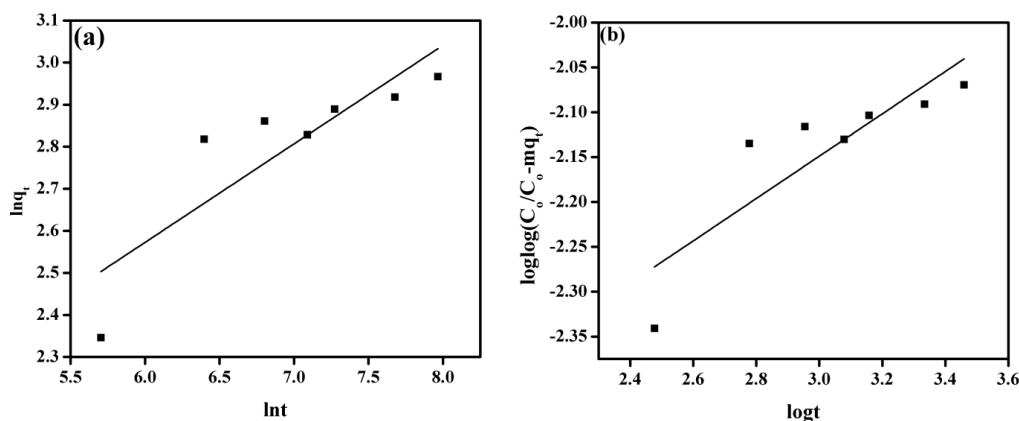


Fig. 8. (a) Modified Freundlich equation plot of $\ln t$ vs. $\ln q_t$ for adsorption of MO and (b) Bangham equation plot of $\log t$ vs. $\log\log(C_0/C_0 - mq_t)$ for adsorption of MO onto the prepared triethanolamine functionalized-AEM.

References

- [1] S.S. Behera, S. Das, B.M. Murmu, R.K. Mohapatra, T.R. Sahoo, P.K. Parhi, Kinetics, Thermodynamics and isotherm studies on adsorption of methyl violet from aqueous solution using activated bio-adsorbent: Phragmites karka, *Curr. Environ. Eng.*, 3 (2016) 229–241.
- [2] R. Xiong, H.S. Kim, S. Zhang, S. Kim, V.F. Korolovych, R. Ma, Y.G. Yingling, C. Lu, V.V. Tsukruk, Template-guided assembly of silk fibroin on cellulose nanofibers for robust nanostructures with ultrafast water transport, *ACS Nano*, 11 (2017) 12008–12019.
- [3] X. Yang, Y. Du, X. Zhang, A. He, Z.-K. Xu, Nanofiltration membrane with a mussel-inspired interlayer for improved permeation performance, *Langmuir*, 33 (2017) 2318–2324.
- [4] S.S. Behera, B.M. Murmu, S. Das, R.K. Mohapatra, B.K. Bindhani, P.K. Parhi, Extensive investigation on the study for the adsorption of Bromocresol Green (BCG) dye using activated Phragmites karka, *Indian J. Chem. Technol.*, 25 (2008) 409–420.
- [5] S. Chen, J. Zhang, C. Zhang, Q. Yue, Y. Li, C. Li, Equilibrium and kinetic studies of methyl orange and methyl violet adsorption on activated carbon derived from Phragmites australis, *Desalination*, 252 (2010) 149–156.
- [6] R.K. Mohapatra, P.K. Parhi, S. Pandey, B.K. Bindhani, H. Thatoi, C.R. Panda, Active and passive biosorption of Pb(II) using live and dead biomass of marine bacterium *Bacillus xiamenensis* PbRPSD202: kinetics and isotherm studies, *J. Environ. Manage.*, 247 (2019) 121–134.
- [7] K.H. Park, P.K. Parhi, N.-H. Kang, Studies on removal of low content copper from the sea nodule aqueous solution using the cationic resin TP 207, *Sep. Sci. Technol.*, 47 (2012) 1531–1541.
- [8] V. Golob, A. Vinder, M. Simonič, Efficiency of the coagulation/flocculation method for the treatment of dye bath effluents, *Dyes Pigm.*, 67 (2005) 93–97.
- [9] G. Annadurai, L.Y. Ling, J.-F. Lee, Adsorption of reactive dye from an aqueous solution by chitosan: isotherm, kinetic and thermodynamic analysis, *J. Hazard. Mater.*, 152 (2008) 337–346.
- [10] S.S. Azhar, A.G. Liew, D. Suhardy, K.F. Hafiz, M.I. Hatim, Dye removal from aqueous solution by using adsorption on treated sugarcane bagasse, *Am. J. Appl. Sci.*, 2 (2005) 1499–1503.
- [11] M. Tabatabaee, S.A. Mirrahimi, Photodegradation of dye pollutant on Ag/ZnO nanocatalyst under UV-irradiation, *Orient. J. Chem.*, 27 (2011) 65–70.
- [12] S.-H. Joo, Y.-U. Kim, J.-G. Kang, J.R. Kumar, H.-S. Yoon, P.K. Parhi, S.M. Shin, Recovery of rhenium and molybdenum from molybdenite roasting dust leaching solution by ion exchange resins, *Mater. Trans.*, 53 (2012) 2034–2037.
- [13] Y. Liu, Y. Zheng, A. Wang, Enhanced adsorption of Methylene Blue from aqueous solution by chitosan-g-poly(acrylic acid)/vermiculite hydrogel composites, *J. Environ. Sci.*, 22 (2010) 486–493.
- [14] H. Deng, J. Lu, G. Li, G. Zhang, X. Wang, Adsorption of methylene blue on adsorbent materials produced from cotton stalk, *Chem. Eng. J.*, 172 (2011) 326–334.
- [15] S. Karcher, A. Kornmüller, M. Jekel, Screening of commercial sorbents for the removal of reactive dyes, *Dyes Pigm.*, 51 (2001) 111–125.
- [16] S. Karcher, A. Kornmüller, M. Jekel, Anion exchange resins for removal of reactive dyes from textile wastewaters, *Water Res.*, 36 (2002) 4717–4724.
- [17] M.I. Khan, M.H. Lashari, M. Khraisheh, S. Shahida, S. Zafar, P. Prapamonthon, A. Rehman, S. Anjum, N. Akhtar, F. Hanif, Adsorption kinetic, equilibrium and thermodynamic studies of Eosin-B onto anion exchange membrane, *Desal. Water Treat.*, 155 (2019) 84–93.
- [18] M.I. Khan, T.M. Ansari, S. Zafar, A.R. Buzdar, M.A. Khan, F. Mumtaz, P. Prapamonthon, M. Akhtar, Acid green-25 removal from wastewater by anion exchange membrane: adsorption kinetic and thermodynamic studies, *Membr. Water Treat.*, 9 (2018) 79–85.
- [19] M.I. Khan, M.A. Khan, S. Zafar, M.N. Ashiq, M. Athar, A.M. Qureshi, M. Arshad, Kinetic, equilibrium and thermodynamic studies for the adsorption of methyl orange using new anion exchange membrane (BII), *Desal. Water Treat.*, 58 (2017) 285–297.
- [20] M.I. Khan, S. Zafar, M.A. Khan, A.R. Buzdar, P. Prapamonthon, Adsorption kinetic, equilibrium and thermodynamic study for the removal of Congo Red from aqueous solution, *Desal. Water Treat.*, 98 (2017) 294–305.
- [21] N. Li, T. Yan, Z. Li, T. Thurn-Albrecht, W.H. Binder, Comb-shaped polymers to enhance hydroxide transport in anion exchange membranes, *Energy Environ. Sci.*, 5 (2012) 7888–7892.
- [22] M.I. Khan, A.N. Mondal, B. Tong, C. Jiang, K. Emmanuel, Z. Yang, L. Wu, T. Xu, Development of BPPO-based anion exchange membranes for electro dialysis desalination applications, *Desalination*, 391 (2016) 61–68.
- [23] M.I. Khan, C. Zheng, A.N. Mondal, M.M. Hossain, B. Wu, K. Emmanuel, L. Wu, T. Xu, Preparation of anion exchange membranes from BPPO and dimethylethanolamine for electro dialysis, *Desalination*, 402 (2017) 10–18.
- [24] M.I. Khan, R. Luque, P. Prinsen, A. Rehman, S. Anjum, M. Nawaz, A. Shaheen, S. Zafar, M. Mustaqeem, BPPO-based anion exchange membranes for acid recovery via diffusion dialysis, *Materials*, 10 (2017), doi: 10.3390/ma10030266.
- [25] M.I. Khan, R. Luque, S. Akhtar, A. Shaheen, A. Mehmood, S. Idress, S. Buzdar, A. Rehman, Design of anion exchange membranes and electro dialysis studies for water desalination, *Materials*, 9 (2016) 1–14, doi: 10.3390/ma9050365.
- [26] A. Kumar, V. Kumar, P.K. Sain, M. Kumar, K. Awasthi, Synthesis and characterization of polyaniline membranes with secondary amine additive containing N,N'-dimethyl propylene urea for fuel cell application, *Int. J. Hydrogen Energy*, 43 (2018) 21715–21723.
- [27] M.I. Khan, Comparison of different quaternary ammonium groups on desalination performance of BPPO-based anion exchange membranes, *Desal. Water Treat.*, 108 (2018) 49–57.
- [28] M.I. Khan, J. Su, E. Lichtfouse, L. Guo, Higher efficiency of triethanolamine-grafted anion exchange membranes for acidic wastewater treatment, *Desal. Water Treat.*, 197 (2020) 41–51.
- [29] M.I. Khan, L. Wu, A.N. Mondal, Z. Yao, L. Ge, T. Xu, Adsorption of methyl orange from aqueous solution on anion exchange membranes: adsorption kinetics and equilibrium, *Membr. Water Treat.*, 7 (2016) 23–38.
- [30] M.A. Khan, M.I. Khan, S. Zafar, Removal of different anionic dyes from aqueous solution by anion exchange membrane, *Membr. Water Treat.*, 8 (2017) 259–277.
- [31] T. Xu, W. Yang, Fundamental studies of a new series of anion exchange membranes: membrane preparation and characterization, *J. Membr. Sci.*, 190 (2001) 159–166.
- [32] C.G. Arges, L. Wang, M.-S. Jung, V. Ramani, Mechanically stable poly(arylene ether) anion exchange membranes prepared from commercially available polymers for alkaline electrochemical devices, *J. Electrochem. Soc.*, 162 (2015) F686–F693.
- [33] M.I. Khan, A.N. Mondal, K. Emmanuel, M.M. Hossain, N.U. Afsar, L. Wu, T. Xu, Preparation of pyrrolidinium-based anion-exchange membranes for acid recovery via diffusion dialysis, *Sep. Sci. Technol.*, 51 (2016) 1881–1890.
- [34] Y. Li, T. Xu, M. Gong, Fundamental studies of a new series of anion exchange membranes: membranes prepared from bromomethylated poly(2,6-dimethyl-1,4-phenylene oxide) (BPPO) and pyridine, *J. Membr. Sci.*, 279 (2006) 200–208.
- [35] N. Tahir, H.N. Bhatti, M. Iqbal, S. Noreen, Biopolymers composites with peanut hull waste leachate and application for Crystal Violet adsorption, *Int. J. Biol. Macromol.*, 94 (2017) 210–220.
- [36] S. Mohan, R. Gandhimathi, Removal of heavy metal ions from municipal solid waste leachate using coal fly ash as an adsorbent, *J. Hazard. Mater.*, 169 (2009) 351–359.
- [37] P.P. Rath, B. Priyadarshini, S.S. Behera, P.K. Parhi, S.R. Panda, T.R. Sahoo, Adsorptive removal of Congo Red Dye from aqueous solution using TiO₂ nanoparticles: kinetics, thermodynamics and isothermal insights, *AIP Conf. Proc.*, 2115 (2019) 1–5, doi: 10.1063/1.5112954.

- [38] S. Zafar, M.I. Khan, M. Khraisheh, M.H. Lashari, S. Shahida, M.F. Azhar, P. Prapamonthon, M.L. Mirza, N. Khalid, Kinetic, equilibrium and thermodynamic studies for adsorption of nickel ions onto husk of *Oryza sativa*, *Desal. Water Treat.*, 167 (2019) 277–290.
- [39] Y.-S. Ho, Second-order kinetic model for the sorption of cadmium onto tree fern: a comparison of linear and non-linear methods, *Water Res.*, 40 (2006) 119–125.
- [40] S. Sinha, S.S. Behera, S. Das, A. Basu, R.K. Mohapatra, B.M. Murmu, N.K. Dhal, S.K. Tripathy, P.K. Parhi, Removal of Congo Red dye from aqueous solution using Amberlite IRA-400 in batch and fixed bed reactors, *Chem. Eng. Commun.*, 205 (2018) 432–444.
- [41] S.S. Behera, S. Das, P.K. Parhi, S.K. Tripathy, R.K. Mohapatra, M. Debata, Kinetics, thermodynamics and isotherm studies on adsorption of methyl orange from aqueous solution using ion exchange resin Amberlite IRA-400, *Desal. Water Treat.*, 60 (2017) 249–260.
- [42] M. Özacar, İ.A. Şengil, A kinetic study of metal complex dye sorption onto pine sawdust, *Process Biochem.*, 40 (2005) 565–572.
- [43] S. Chowdhury, R. Mishra, P. Saha, P. Kushwaha, Adsorption thermodynamics, kinetics and isosteric heat of adsorption of malachite green onto chemically modified rice husk, *Desalination*, 265 (2011) 159–168.
- [44] E. Tütem, R. Apak, Ç.F. Ünal, Adsorptive removal of chlorophenols from water by bituminous shale, *Water Res.*, 32 (1998) 2315–2324.
- [45] I.D. Mall, V.C. Srivastava, N.K. Agarwal, I.M. Mishra, Adsorptive removal of malachite green dye from aqueous solution by bagasse fly ash and activated carbon-kinetic study and equilibrium isotherm analyses, *Colloids Surf., A*, 264 (2005) 17–28.